Targeted conversion of protein and glucose waste streams to volatile fatty acids by metabolic models

A. Regueira, R. Bevilacqua, J. M. Lema, M. Carballa, M. Mauricio-Iglesias

**Department of Chemical Engineering, Institute of Technology, Universidade de Santiago de Compostela, Spain (e-mail: alberte.regueira@usc.es).*

Abstract: Mixed-culture fermentations are recognised as suitable processes to valorise organic wastes and convert them into added-value products. One of the main issues of these processes is that the stoichiometry of the fermentations is highly dependent on operational conditions such as the pH or the concentrations of the different substrates. In this work we developed a mathematical model for the production of volatile fatty acids from wastes featuring high concentrations of carbohydrates and proteins. The model reproduces experimental results, predicting the tendencies of the product spectrum when varying pH values and at different proportions of carbohydrates and proteins in the feeding. This model can be the core of a tool for the computer-aided design of mixed-culture fermentations.

Keywords: metabolic modelling; mixed microbial cultures; computer-aided process design; volatile fatty acids production; anaerobic cofermentation.

1. INTRODUCTION

Anaerobic mixed-culture fermentations (MCF) are processes yielding a mixture of volatile fatty acids (VFA), which are valuable on their own as chemicals. Alternatively, VFA can be used as substrate in subsequent bioprocesses to yield high added-value products (e.g. bioplastics) in a biorefinery production scheme (Agler et al., 2011). In this way, MCF are postulated as valid processes to valorise organic residues. Using mixed cultures of microorganisms gives the process substantial economic and operational advantages (e.g. no need for sterilisation and therefore the possibility of continuous processes) but also poses additional challenges in comparison with the use of pure cultures. The behaviour of mixed cultures is still not well controlled, which makes the design of processes based on MCF a difficult task. One of the main limitations of the process is that the product spectrum varies significantly with the operational conditions (pH, HRT, feeding). Although this opens the possibility of directing the process by varying these conditions, it also makes process design and optimisation only possible at the expense of a large number of experimental trials. In this sense, metabolic energy-based models have been able to explain mechanistically the product spectrum of MCF and can be useful tools for predicting the stoichiometry of MCF (González-Cabaleiro et al., 2015). This modelling approach assumes that the selective pressure in energy-constrained environments favours those microorganisms capable of harvesting the maximum energy from the substrate. As a consequence, the expected product spectrum would be governed by pathways associated with a high ATP yield. Glucose and protein MCF were successfully simulated using this approach (González-Cabaleiro et al., 2015; Regueira et al., submitted for publication). The effect of pH on the product spectrum was of special interest since it has a major effect on the outcome of such processes and it is one of the few design variables that we can manipulate.

This work is framed in the ERA-IB-2 project BIOCHEM, with the goal of proposing a design methodology for the conversion of different fractions of organic wastes (i.e. carbohydrates, proteins and lipids) into VFA. Usually, real organic wastes are composed of more than one fraction as for example dairy or certain canning industry wastes, which feature carbohydrates and proteins. It was shown in the aforementioned protein model that the different amino acids (AA) competed for shared resources (i.e. electron equivalents) and that their relative concentrations were a key factor determining the outcome of these interactions. Our hypothesis is that glucose and protein fractions would also interact with each other in a co-substrate fermentation. As a result, the stoichiometry of the process would be different than the addition of the monofermentation stoichiometries of glucose and protein.

The objective of this work is to develop a metabolic model for the production of VFA from the cofermentation of protein and glucose by mixed cultures of microorganisms. We intend to predict the stoichiometry of VFA production at different pH values and at different proportions of glucose and protein. The goal of such a model is twofold: i) to give insight on the degradation mechanisms and on the interactions between the different substrates and ii) to be used as a design tool for MCF-based processes that convert wastes rich in protein and carbohydrates into VFA.

2. MODEL DESCRIPTION

The model is based on the dynamic mass balances (1-4) of the different compounds (states) in a continuous stirred tank reactor (CSTR), following the framework described by González-Cabaleiro et al. (2015) for glucose MCF. There are 68 states: 24 intracellular compounds, 40 extracellular

compounds in the bulk reactor, 4 gaseous compounds and biomass. The system comprises three compartments: intracellular volume (V_x), reactor volume (V_r), extracellular volume (reactor bulk, V_{liq}) and gas head space (V_{gas}). The mass balances for each of the compartments are defined by the following equations (1-4).

Intracellular compounds

$$\frac{dS_i}{dt} = R_i + R_{T,i} \quad (1)$$

Where S_i is the concentration (mol L_x^{-1}), R_i and $R_{T,i}$ are, respectively, the reaction rate and intra-extra cellular transport rate (mol L_x^{-1} h^{-1}).

Extracellular compounds

$$\frac{dS_k}{dt} = D_{liq} \cdot \left(S_{K,in} - S_k\right) + R_{T,k} \quad (2)$$

Where S_k is the concentration (mol L_{liq}^{-1}), D_{liq} is the liquid dilution rate (h^{-1}) $R_{T,j}$ is the intra-extra cellular transport rate (mol L_{liq}^{-1} h^{-1}).

Biomass

$$\frac{dS_X}{dt} = -D_{liq} \cdot S_X + R_{ana} - R_{decay} \quad (3)$$

Where S_X is the biomass concentration (mol L_r^{-1}) and R_{ana} and R_{decay} are the anabolism and decay rate (mol L_r^{-1} h^{-1}).

Gas compounds

$$\frac{dG_m}{dt} = -D_{gas} \cdot G_m + R_{T,m} \quad (4)$$

Where G_m is the concentration (mol L_{gas}^{-1}), D_{gas} is the headspace dilution rate (h^{-1}) and $R_{T,m}$ is liquid-gas transport rate (mol L_{gas}^{-1} h^{-1}).

Protein hydrolysis is omitted in the model and is directly considered a mixture of AA. Therefore, the substrate for this system is composed by glucose and AA. Intracellular substrate concentrations are assumed constant at a value of 0.1 mM following our framework. There are 119 possible reactions, resulting in a 68x119 metabolic network matrix. Amongst all the reaction rates 22 of them are independent, i.e. depending solely on extracellular concentrations.

2.1 Metabolic network

Glucose degradation pathways include conversion to acetate, propionate, butyrate, ethanol and lactate as reported in Regueira *et al.* (2018). There are 17 AA considered in the metabolic network: alanine (Ala), arginine (Arg), asparagine (Asn), aspartate (Asp), cysteine (Cys), glutamate (Glu), glutamine (Gln), glycine (Gly), histidine (His), isoleucine (Ile), leucine (Leu), lysine (Lys), methionine (Met), proline (Pro), serine (Ser), threonine (Thr) and valine (Val). Their considered end products in this network are: acetate, propionate, iso-butyrate, n-butyrate, iso-valerate, n-valerate, iso-caproate and ethanol. The catabolism of AA is remarkably varied. Some AA can only yield one product (Gly can only be converted to acetate) while others can have as much as five different end products (Arg can be converted to acetate, propionate, butyrate, ethanol and/or n-valerate). Among all the possible conversion pathways for each of the different AA, we included in the metabolic network those most often reported in literature for anaerobic AA degraders.

Two electron carrier (EC) couples are considered in the network: ferredoxin (Fd_{red}/Fd_{ox}) and $NADH/NAD^+$. The ferredoxin couple is only related to high energy metabolic steps such as decarboxylations (as in pyruvate conversion to acetyl-CoA) and is considered to be oxidised producing H_2 or formate. On the contrary, the couple $NADH/NAD^+$ has to be balanced among the metabolic pathways. NAD^+ to NADH ratio is set fixed to a value of 10.

2.2 Model hypotheses

Fermentations carried out in CSTR are low-energy environments (LaRowe et al., 2012) and it is expected that microorganisms perform pathway with high ATP yield. Therefore, it is expected that kinetic differences among the different pathways consuming a particular substrate do not have a strong influence on the pathway selection.

Protein consumption is generally slower than glucose consumption, as shown in literature (Breure et al., 1986), which could influence the process stoichiometry. In environments with reactions close to the thermodynamic equilibrium the flux is positively correlated with the Gibbs free energy (ΔG) of the reaction. The ratio between the maximum consumption rate of glucose and of protein was set equal to the ratio between the average ΔG at standard biological conditions (pH 7 and metabolic concentration of 1 mM) of all the featured glucose degradation pathways and all the AA degradation pathways, normalised by the number of steps on each pathway (5). Glucose pathways have on average a 50% higher absolute value of ΔG than those of AA degradation. Therefore, glucose maximum consumption rate coefficient in the Monod equation was set 50% higher than that of the AA. We consider the maximum uptake rate as 0.75 mol L_x^{-1} h^{-1} for glucose and 0.50 mol L_x^{-1} h^{-1} for all the AA. The affinity constant is set equal for all substrates at 1 mM.

$$\frac{q_{Glucose}^{max}}{q_{protein}^{max}} = \frac{\frac{1}{n_{Glucose}} \cdot \sum_i \frac{\Delta G'^m_{glucose,i}}{k_{glucose,i}}}{\frac{1}{n_{AA}} \cdot \sum_j \sum_k \frac{\Delta G'^m_{AA\ j,k}}{k_{AA\ j,k}}} = 1.5 \quad (5)$$

Where q^{max} is the maximum consumption rate, $\Delta G'^m$ is the reaction Gibbs free energy at standard biological conditions, k is the number of metabolic steps and n is the number of pathways. The subscript i, j and k denote the different glucose conversion pathways, the different AA and their different conversion pathways, respectively.

This model follows an "enzyme soup" approach for describing the microbial community structure. In this way a virtual microorganism containing all the metabolic functions is assumed. This approach is more appropriate than a compartmentalised one when the a priori knowledge about the microbial consortia is limited and the system is open to new microorganisms (Biggs et al., 2015). Moreover, it proved to be

capable of good predictions for MCF of glucose (González-Cabaleiro et al., 2015) and proteins (Regueira et al., unpublished). In our case, when having a mixed substrate feeding, an "enzyme soup" approach is also valid as the environmental conditions (low substrate concentration typical of CSTR operations) favour the presence of generalist microorganisms over specialist ones (Kuenen, 1983).

The different substrates might not be consumed due to energetic or thermodynamic reasons: if the conversion pathways of a substrate are all endergonic or if converting one substrate is detrimental for the global energy harvest rate. This limitation is expressed in the model as a variable uptake ratio for each of the substrates.

2.3 Solution strategy

The different terms of the balances are determined following the flowchart shown in Fig. 1. The initial states values and the feeding characteristics are the initial inputs of the model. Firstly, in the reaction selection step all the possible conversion pathways of each of the substrates are evaluated. The reaction evaluation step is divided into several substeps: determination of the reaction rates (Kinetics), of the associated transport rates (Transport) and of the ATP production rate by proton translocations and active transport (Energetics). First these tasks are evaluated assuming that each of the substrates is totally converted through each the possible degradation pathways. Secondly, the optimal set of reactions is selected in the Optimisation by linear optimisation (6-9). Then, the Kinetics, Transport and Energetics substeps are repeated in the main workflow line to evaluate the set of pathways deemed as optimal. Finally, the mass balances (1-4) are determined and the steady state condition is evaluated. If it is not yet reached, the state values are updated following a pseudo-time stepping solution procedure and a new iteration begins.

The objective function aims to maximise the global ATP production from the substrates. The net ATP production includes the ATP formed by substrate-level phosphorylation, the ATP gained through proton translocations and the ATP spent in the active transport of compounds. The solution is constrained by NADH conservation: its production and consumption must be balanced within the catabolism because there is no external electron acceptor that could act as an electron sink. Thus, the optimisation problem to be solved can be expressed as follows (6-9):

$$\max_{z} \quad r_{ATP}(z) \qquad \text{(mol ATP/Lx·h)} \qquad (6)$$

$$r_{NADH}(z) = 0 \qquad \text{(mol NADH/Lx·h)} \qquad (7)$$

$$0 \le z_{i,j} \le 1 \qquad (8)$$

$$\sum_{j} z_{i,j} = 1\,, \quad i = 1, \dots, nAA \qquad (9)$$

Where: r_{ATP} and r_{NADH} are the global ATP and NADH production rates, respectively and $z_{i,j}$ are the elements of the matrix of decision variables. They represent the yield of the different metabolic branches of the different substrates. Concretely, $z_{i,j}$ is the yield of the metabolic branch i of the jth substrate and varies continuously between 0 and 1. For each of the substrates there is a branch representing a null reaction.

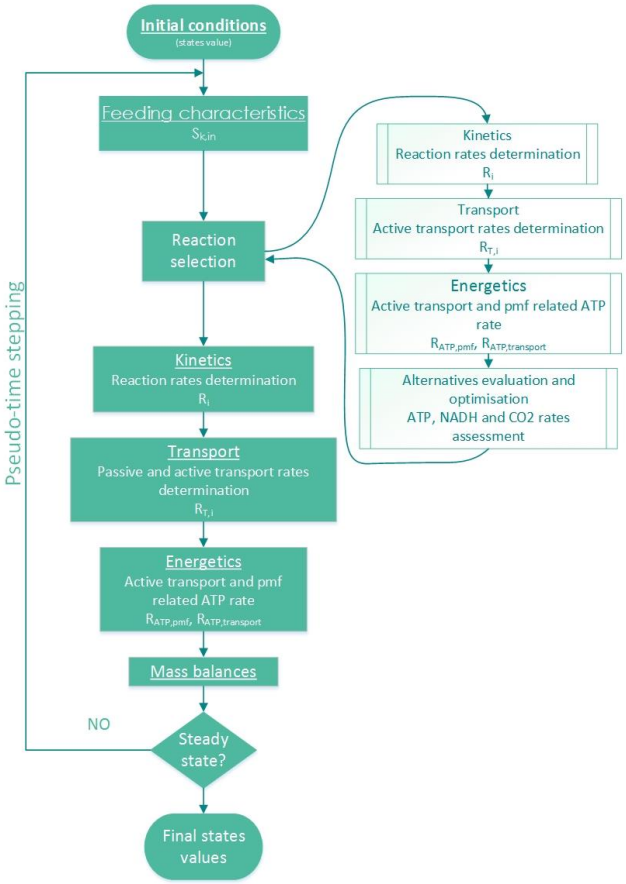

Fig. 1. Workflow diagram for model solution

The model of the reactor can be solved to steady state as a system of 68 nonlinear algebraic equations. Testing Newton-based methods for the solution of the system of nonlinear algebraic equations, we observed a tendency to get stuck in local solutions or be driven to infeasible states (e.g. negative concentrations). To prevent these issues, we used pseudo-time stepping as heuristic solving method as previously reported by Ceze and Fidkowski (2015), whereby the algebraic system of equations is formulated as a system of ODEs. This system of ODEs was solved until steady state by the Matlab command ode15s. Steady state was assumed when all the state absolute derivatives values were under 1e-6 mol L^{-1} h^{-1}. Although based in FBA strategies, our approach differs in how internal concentrations are assumed. Usually in FBA, measured internal concentration values at steady state are used or determined by heuristic (e.g. the most probable values based on maximum compatible metabolic concentration, energetics as in Rodriguez *et al.* 2006)). This assumption limits the influence of environmental conditions on the product spectrum because it fixes most of the intracellular concentrations to a set value. However, our approach focuses on studying how environmental conditions are linked to the intracellular environment and vice versa through energy-related mechanisms such as active transport across the membrane or the energy gathered through proton translocations.

3. RESULTS AND DISCUSSION

A CSTR was simulated with a dilution rate (D) of 0.1 h^{-1} for a range of pH values (from 4 to 8.5 with 0.5 increments) and for a range of concentrations of a protein (gelatine) and a carbohydrate (glucose) from 0 to 10 g/L (with 1 g/l increments, keeping a total feeding concentration of 10 g/L). Simulation results show that the yields of the different VFA are affected by both the pH value and the glucose to protein ratio. For example, n-butyrate yield is higher when pH is low and at high glucose to protein ratios, attaining a maximum value of 0.4 g n-butyrate/g substrate (Fig. 2). Other VFA are affected differently: n-valerate yield is favoured at low glucose to protein ratio and is generally not affected by pH. Conversion is also affected and ranged from 99.8%, when glucose was the only carbon source and at high pH, to 84.5% when gelatine was the only substrate and at low pH. These values should be interpreted as the maximum values from a thermodynamic point of view, as the model does not consider any kinetic inhibition affecting substrate conversion.

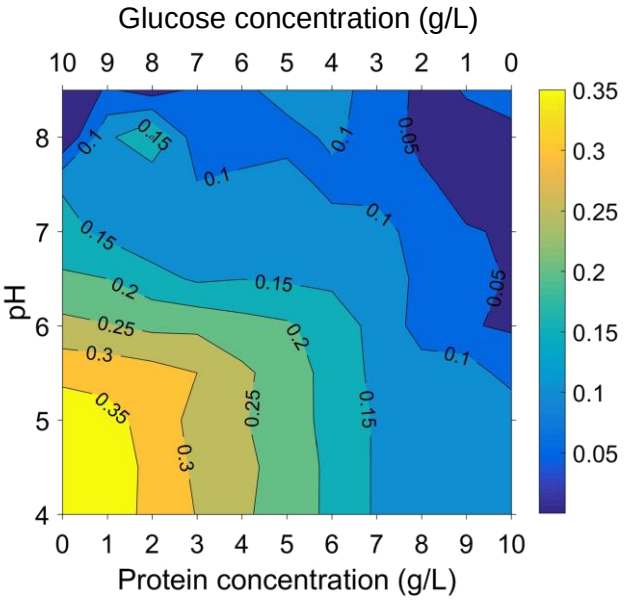

Fig. 2. Predicted n-butyrate yields (g/g of feeding) at different pH values (vertical axis) and at different glucose and gelatine concentrations in the feeding (horizontal axis).

The model allows to explore the operational space of two parameters (pH and glucose/protein fractions). In this way, the information provided by the model is of great interest when aiming at designing a process as it makes possible to target a specific VFA with a high selectivity, given that a sufficient number of waste streams are available.

3.1 Mechanistic insight

This section shows the information that can be obtained from the model simulations and how it can explain the different trends observed on VFA yields, focusing on the effect of cofermenting substrates. The yield of n-butyrate is clearly affected by the relative concentration of glucose and protein. For example, at pH 6.5 its yield varies from 0.26 g/g (for 10 g/L of glucose and 0 g/L of protein) to 0.05 g/g (for 0 g/L of glucose and 10 g/L of protein). This behaviour is directly explained by glucose concentration in the feeding (Fig. 3): its yield on butyrate increases when its concentration is high in the feeding (green bars in Fig. 3) and acetate yield, on the contrary, is higher at high protein concentrations (blue bars are bigger than green bars in the right part of Fig. 3). At high protein concentrations glutamate yield on butyrate is high (red bars in Fig. 3) but the overall butyrate yield is lower in these conditions (Fig. 2) because glutamate only represent 17% of the protein mass and therefore its conversion stoichiometry has a limited impact on the overall VFA yields.

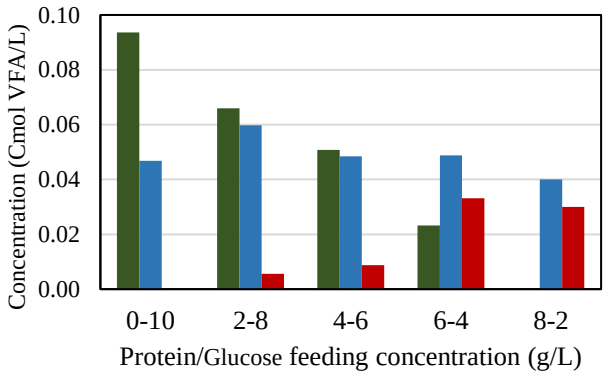

Fig. 3. Butyrate and acetate concentration (Cmol/L) due to glucose and glutamate conversion at pH 6.5 and at different feeding proportions. ■ butyrate from glucose ■ acetate from glucose ■ butyrate from glutamate.

Glucose conversion to acetate is the most favourable pathway as it has the highest ATP rate among the other options (Table 1, reactions 1-3). However, it leads to a net NADH production that must be consumed in other pathways. Therefore, if glucose is degraded on its own, it cannot only produce acetate. But, when glucose is converted simultaneously with AAs, this NADH surplus can be absorbed in other pathways and in consequence glucose is completely transformed into acetate when the protein concentration is high enough (Fig. 3). In the intermediate cases, there is an equilibrium between transforming glucose through its most energetic pathway and the NADH absorption capacity of other pathways. For example, in the conditions of Table 1, converting glucose to butyrate has an ATP rate 44% lower than yielding acetate, with an opportunity cost of 0.24 mol ATP/mol NADH (i.e. for each NADH produced in the acetate pathway, 0.24 extra ATP are produced). To accommodate the extra NADH produced by glucose some AAs are rerouted through pathways with a lower ATP production. For example, glutamate is partially converted to butyrate (reaction 4) when its conversion to acetate has a 31% higher ATP generation rate, with an opportunity cost of 0.24 mol ATP/mol NADH. These two changes in conversion pathways are in fact in equilibrium as they have the same value of opportunity cost (i.e. the extra ATP rate harvested in glucose conversion to acetate instead of butyrate is lost in glutamate conversion to butyrate instead to acetate). Other AAs have their conversion pathways completely switched as, for example, isoleucine and valine, which are AA that always produce NADH. As their opportunity cost is lower than that of glucose conversion to butyrate instead of acetate, they are left unconsumed (reactions 8 and 9). Alanine, however, does not change its conversion pathway (reactions 6 and 7) because the opportunity cost of changing it is higher than that of glucose and

therefore it is not globally worthwhile to convert it to propionate instead of to butyrate.

Table 1. Steady state solution for pH 6.5, glucose concentration of 6 g/L and protein concentration of 4 g/L. r_{ATP} and r_{NADH} are the intracellular rates of ATP and NADH (mol L_x^{-1} h^{-1}).

#	Reaction	Z	r_{ATP}	r_{NADH}	Opportunity cost*
1	Glucose→ But	0.43	0.317	0	0.24
2	Glucose→ 2Ac	0.41	0.458	0.580	
3	Glucose→2 Pro	0.16	0.176	-0.580	
4	Glutamate→But	0.41	0.019	-0.05	0.24
5	Glutamate→2Ac	0.59	0.032	0	
6	Alanine→Pro	0	-0.004	-0.019	0.28
7	Alanine→But	0.99	0.001	0	
8	Isoleucine→iVal	0	0.129	0.852	0.15
9	Valine→iBut	0	0.176	1.158	0.15

*Opportunity cost is defined as the difference in r_{ATP} divided by the difference in r_{NADH} between two pathways.

3.2 Comparison with experimental data

We chose one experimental data set from literature (Breure et al., 1986) as representative since the product spectrum is reported in detail and methanisation is completely discarded. In these experiments, glucose (10 g/L) was added to the feeding of a CSTR after being fed only gelatine (5 g/L) until stabilisation at a D of 0.10, 0.15 and 0.20 h^{-1}. Simulations were done mimicking the different conditions of these experiments in both mono and cofermentation scenarios (Fig. 4). Even though the experimental results show significant deviations in some cases (especially in cofermentation results), these deviations do not follow a patter with the value of D and therefore we decided to represent the average values for the sake of simplicity.

The model predicts relatively well the product spectrum both in cofermentation and monofermentation experiments. Moreover, it is able to capture most part of the changes in product spectrum by the addition of glucose to the feeding (Fig. 4). The iso forms of butyrate and valerate disappear from the product spectrum during cofermentation experiments, n-butyrate yield increases significantly when glucose is present as well as the yield of ethanol. Propionate yield value does not change between mono and cofermentation in both the experimental data and the model results, but a considerable deviation is present on the cofermentation experimental data. Propionate is always overpredicted by the model, which could be partially explained by a mismatch between the AA profiles of the gelatine used in the model and in the experiments as propionate is yielded by a limited number of AA. The change in n-valerate yield is well foreseen but the actual yields are underpredicted. Since it only can be yielded by two AA (arginine and proline) a difference in the gelatine AA profiles could be also de explanation. Acetate yield decreases in cofermentation in both simulated and experimental data and is overall well predicted.

The experimental results show a significant decrease in protein acidification when glucose is added to the feeding (from an average value of 75% to 20%). This decrease in conversion is not captured by the model and global protein conversion only drops from 91% to 85% in the cofermentation simulations. Non-hydrolysed protein could have prevented the prevalence of generalist microorganisms and together with a relatively high D value it could explain why protein acidification was severely affected by glucose presence (Breure et al., 1986). This model does not consider kinetic inhibition and therefore is not capable of reproducing these events.

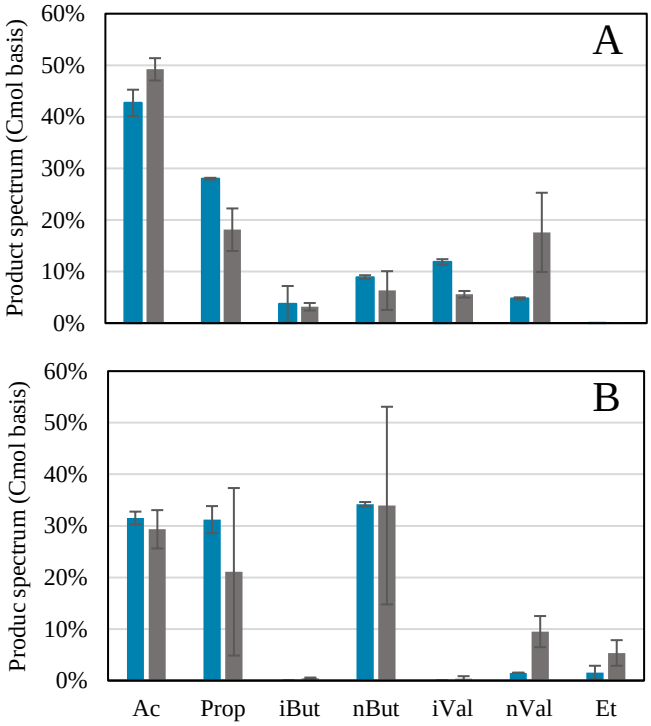

Fig. 4. Product spectra of model and literature results at 3 different D. A: gelatine monofermentation, B: cofermentation. ■ Model results ■ Literature results (Breure et al., 1986).

3.3 Sources of uncertainty

The NADH restriction is modelled assuming that it is fulfilled in common by protein and glucose reactions as we model the community as a generalist. This means that glucose or protein consuming reactions on their own can be non-neutral in terms of NADH. However, if specialist microorganisms dominate the culture, it would be more reasonable to consider that each substrate has an independent NADH conservation restriction, which would affect the conversion stoichiometry. However, as pointed out in section 2.2, in the conditions modelled (low substrate concentration typically found in CSTR), we do expect the prevalence of a generalist microbial community and the experimental data analysed proves indeed this hypothesis valid.

The ratio between the maximum consumption rate of glucose and AA was determined based on the assumption that a more thermodynamically favoured reaction is faster. Reliable data that would have allowed us to determine more accurately this ratio were not available in literature. However, if this parameter is varied 50%, the main VFA yields vary less than 10% on average, which shows a smaller sensitivity than, for example, the proportion between glucose and gelatine (Fig. 2).

3.4 Use as product design tool

The utility of the model developed as a process design tool was already proven when used to explore the operational parameter space. With that information, we could steer the process towards the yield maximisation of determined VFA, when a significant amount of wastes is available. Nonetheless, this model can also be used to design processes that valorise concrete waste streams and to decide which stream is more adequate for our purposes. Cheese whey (CW) or canning industry wastewater are examples of waste streams with a high content of proteins and carbohydrates. As a proof of concept, the conversion of these two waste streams to VFA at different pH values is simulated (tuna cooking wastewater (TCWW) with 7.3 g/L of gelatine and 0.85 g/L of glucose and CW with 1 g/L of casein and 4 g/L of glucose).

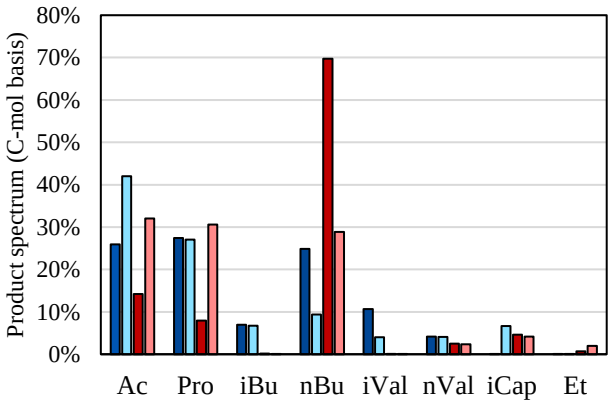

Fig. 5. Model results for TCWW and CW fermentation at D=0.1 h^{-1}. Dark and light colours represent results at pH 5 and 7, respectively. ■ TCWW ■ CW.

As the relative concentration of glucose and protein are different and the waste streams feature different proteins, both the stoichiometry and the pH effect is different. CW product spectrum is dominated by butyrate due to the high proportion of glucose. TCWW has a higher yield on acetate and in general the pH effect on the conversion stoichiometry is less pronounced. This opens the possibility of choosing beforehand the most interesting waste depending on the targeted VFA. If we are interested in high acetate or propionate production, we would choose TCWW at neutral pH. On the other hand, if butyrate is our targeted VFA, CW at low pH is our best option between these two agro-industrial waste streams.

4. CONCLUSIONS

A mechanistic model for the cofermentation of proteins and glucose by mixed cultures of microorganisms was developed and reproduces satisfactorily both the expected product spectrum and the effect of adding glucose to a gelatine fermentation. The model shows that glucose to protein ratio in the feeding affects the conversion pathways selected by the model, owing to competition for shared resources (i.e. NADH). In this way, the design process counts with an extra degree of freedom, as mixtures of glucose and protein can be tailored to direct the process towards the desired VFA. The model was only partially validated as only few well-designed experiments are available in literature. Expressly designed experiments tracking glucose and individual amino acids conversions are being run to complete the validation of the model and the more general process design methodology. Overall, this model, together with a standard kinetic model, will be used as a tool for the early stage design of processes degrading mixtures of carbohydrates and proteins anaerobically by mixed cultures of microorganisms.

ACKNOWLEDEMENTS

The authors would like to acknowledge the support of the Spanish Ministry of Education (FPU14/05457) and ERA-IB-2 project BIOCHEM (PCIN 2016-102) funded by MINECO. The authors belong to the Galician Competitive Research Group ED431C2017/029 and to the CRETUS Strategic Partnership (ED431E 2018/01), both programmes are co-funded by FEDER (UE).

REFERENCES

Agler, M.T., Wrenn, B.A., Zinder, S.H., Angenent, L.T., (2011). Waste to bioproduct conversion with undefined mixed cultures: the carboxylate platform. *Trends Biotechnol* 29, 70–78.

Biggs, M.B., Medlock, G.L., Kolling, G.L., Papin, J.A., (2015). Metabolic network modeling of microbial communities. *Wiley Interdisciplinary Reviews: Systems Biology and Medicine* 7, 317–334.

Breure, A.M., Mooijman, K.A., van Andel, J.G., (1986). Protein degradation in anaerobic digestion: influence of volatile fatty acids and carbohydrates on hydrolysis and acidogenic fermentation of gelatin. *Applied Microbiology and Biotechnology* 24, 426–431.

Ceze, M., Fidkowski, K.J., (2015). Constrained pseudo-transient continuation. *International Journal for numerical methods in Engineering* 102, 1683–1703.

González-Cabaleiro, R., Lema, J.M., Rodríguez, J., (2015). Metabolic Energy-Based Modelling Explains Product Yielding in Anaerobic Mixed Culture Fermentations. *PLoS ONE* 10, e0126739.

Kuenen, J.G., (1983). The Role of Specialists and Generalists in Microbial Population Interactions. In: Blanch, H.W., Papoutsakis, E.T., Stephanopoulos, G. (Eds.), Foundations of Biochemical Engineering. American Chemical Society, pp. 229–251.

LaRowe, D.E., Dale, A.W., Amend, J.P., Van Cappellen, P., (2012). Thermodynamic limitations on microbially catalyzed reaction rates. *Geochimica et Cosmochimica Acta* 90, 96–109.

Regueira, A., González-Cabaleiro, R., Ofițeru, I.D., Rodríguez, J., Lema, J.M., (2018). Electron bifurcation mechanism and homoacetogenesis explain products yields in mixed culture anaerobic fermentations. *Water Research* 141, 5–13.

Regueira, A., Lema, J.M., Carballa, M., Mauricio-iglesias, M., unpublished. Metabolic modelling for predicting VFA production from protein-rich substrates. *Submitted to Biotechnology and Bioengineering*.

Rodriguez, J., Kleerebezem, R., Lema, J.M., van Loosdrecht, M.C., (2006). Modeling product formation in anaerobic mixed culture fermentations. *Biotechnol Bioeng* 93, 592–606.